Aust. J. Math. Anal. Appl.
Vol. **20** (2023), No. 1, Art. 5, 13 pp.
AJMAA

HIGH ORDER COLLOCATION METHOD FOR THE GENERALIZED KURAMOTO-SIVASHINSKY EQUATION

ZANELE MKHIZE, NABENDRA PARUMASUR, AND PRAVIN SINGH

Received 19 January, 2022; accepted 24 January, 2023; published 28 February, 2023.

SCHOOL OF MATHEMATICS, STATISTICS AND COMPUTER SCIENCES, UNIVERSITY OF KWAZULU-NATAL,
PRIVATE BAG X 54001, DURBAN 4000.
mkhizez2@ukzn.ac.za
parumasurn1@ukzn.ac.za
singhp@ukzn.ac.za
URL: https://www.ukzn.ac.za

ABSTRACT. In this paper, we derive the heptic Hermite basis functions and use them as basis functions in the orthogonal collocation on finite elements (OCFE) method. We apply the method to solve the generalized Kuramoto-Sivashinsky equation. Various numerical simulations are presented to justify the computational efficiency of the proposed method.

Key words and phrases: Orthogonal collocation; Heptic Hermite basis; Generalized Kuramoto-Sivashinsky equations.

2010 *Mathematics Subject Classification.* Primary 65L10, 65M70, 65N35.

ISSN (electronic): 1449-5910

1. INTRODUCTION

The Kuramoto-Sivashinsky equation (KSe) is ubiquitous in applications in the nonlinear sciences. It appears in the modelling of spatio-temporal chaos [1, 2, 3]. Originally the equation was used to describe the propagation of waves in dissipative media [4] and in pattern formation and turbulence in flames [5]. It also appears in various important application areas including in a film of viscous liquid flowing down a vertical plane [6] and a thin liquid film on an inclined heated plate [7]. The generalized Kuramoto-Sivashinsky equation (gKSe) has been used in the study of thin viscous film falling down a vertical substrate in the presence of a reactant [8], in the study of dissipative waves in plasma physics [9] and also in the formation of soliton pulses [10]. The theoretical analysis of the Kse and gKSe are well established [2, 3, 11]. In order to model these phenomena successfully highly accurate numerical methods are required which may also be useful in supplementing the theoretical results.

In this paper we consider the numerical solution of the gKSe using a high order collocation method based on C^3 heptic Hermite basis with the collocation points chosen as the Gauss points. Collocation is a useful and versatile numerical method for solving partial differential equations posed on a bounded spatial domain. It is well known that the computational advantages of collocation methods are they are easy to implement, extremely economical and maintain a reasonable degree of accuracy, as compared to the usual finite difference and Galerkin-finite-element numerical schemes. Some classical works on the latter schemes for the periodic case have been proposed in [12, 13] albeit no numerical simulations were furnished. In the paper of [12] they used a Crank-Nicolson-type finite difference method and obtained a method of order 2. In the paper [13] they employed the Galerkin-finite-element method using as the trial space C^1 splines of degree $r-1$ and obtained the optimal spatial rate of convergence r. The use of C^1 splines results in a larger system to be solved as compared to the use of C^3 Hermite splines used here. Many alternative schemes have been proposed and developed using a variety of basis functions such as Lattice Boltzmann method for the generalized Kuramoto-Sivashinsky equation [14], B-splines [15, 16, 17] and cubic Hermite basis functions [18]. In the former case high order schemes have been developed to solve high order PDEs whilst the latter case is usually applied by splitting the original PDE into lower order systems. In this paper, we derive the Hermite heptic basis functions and use them as trial functions to construct a collocation method for solving a fourth order PDE. The method is computationally more efficient than B-splines and there is no need to split the PDE into lower order systems as in the case of cubic Hermite collocation method. The collocation points are chosen as the Gauss points and yields optimal order of convergence which is sometimes referred to as superconvergence (see [19]). Hence, the method is designed to yield orders of convergence similar to the Galerkin method but is computationally more efficient than Galerkin's method since no integrals need to be computed. These methods are referred to as Orthogonal collocation on finite elements (OCFE) [20, 21, 22]. In the present context the use of C^3 heptic Hermite basis functions in the OCFE method yield much smoother and accurate solutions as compared to the methods using C^1 cubic Hermite basis in [23, 24]. In order to illustrate the robustness and versatility of the method we solve the Kuramoto-Sivashinsky and the generalized Kuramoto-Sivashinsky equations.

In Section 2 we derive the heptic Hermite basis and use it to develop the OCFE method in Section 3. In Section 4 we present various numerical examples and simulations. Section 5 concludes the paper.

We do not mention pseudospectral methods based on Chebyshev and Legendre polynomials and Sinc collocation method.

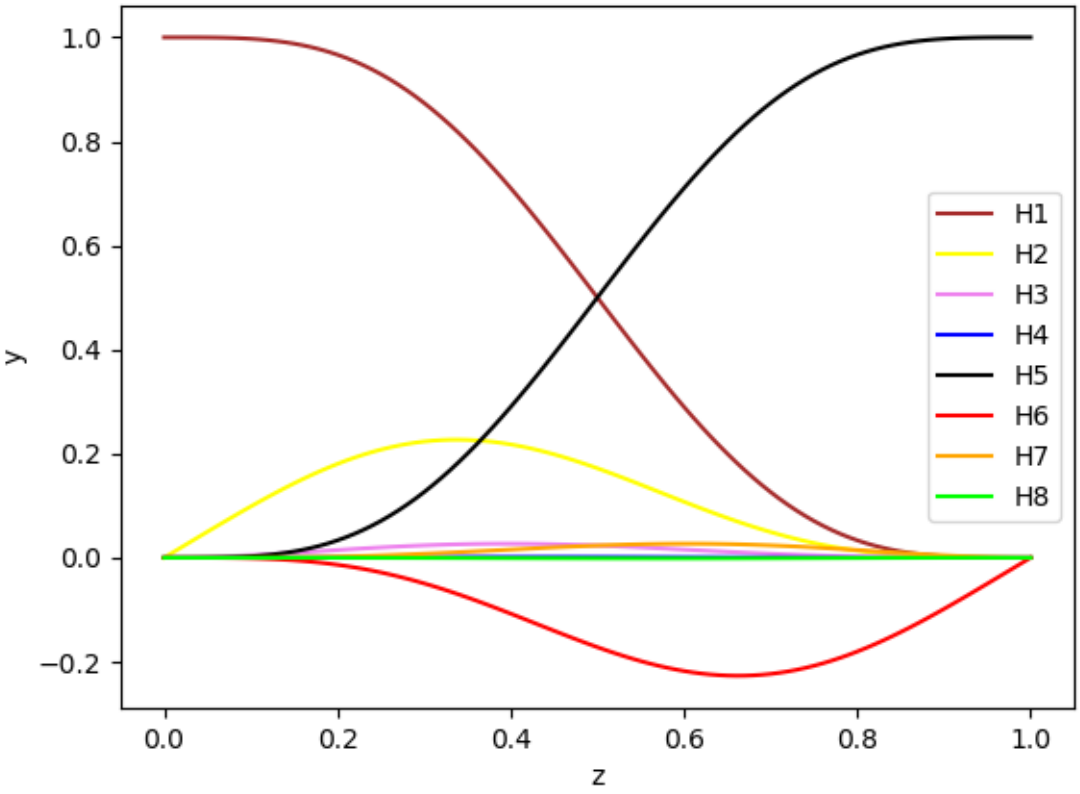

Figure 1: Basis functions

2. HEPTIC HERMITE BASIS

The spatial domain $[a, b]$ is discretized using the partition

$$x_i = a + (i-1)h, \quad i = 1, 2, ...N + 1, \quad h = \frac{(b-a)}{N} \tag{2.1}$$

Each subinterval $[x_i, x_{i+1}]$ is mapped to [0,1] by using the transformation

$$z = \frac{(x - x_i)}{h} \tag{2.2}$$

The interpolating conditions for the heptic basis functions on $[0, 1]$ are given by

$$H_k^{(p)}(0) = H_{k+4}^{(p)}(1) = \delta_{k,p+1} \quad k, p+1 \in S, \text{ where } S = \{1, 2, 3, 4\}$$

These basis functions are illustrated in figure 1.

The derived Hermite polynomials obtained using the above interpolation conditions are:

$$
\begin{aligned}
H_1(z) &= (20z^3 + 10z^2 + 4z + 1)(z-1)^4 \\
H_2(z) &= (10z^3 + 4z^2 + z)(z-1)^4 \\
H_3(z) &= \frac{z^2}{2}(z-1)^4(4z+1) \\
H_4(z) &= \frac{z^3}{6}(z-1)^4 \\
H_5(z) &= H_1(1-z) \\
H_6(z) &= -H_2(1-z) \\
H_7(z) &= H_3(1-z) \\
H_8(z) &= -H_4(1-z)
\end{aligned}
$$

The approximate solution in the i_{th} interval is given by

$$U^i(z,t) = \sum_{k=1}^{8} C_k^{(i)}(t) H_k(z)$$

and in the $(i+1)_{st}$ interval by

$$U^{i+1}(z,t) = \sum_{k=1}^{8} C_k^{(i+1)}(t) H_k(z)$$

By using the continuity of the basis functions and their derivatives up to order 3 at x_{i+1}, we can show that the first four coefficients in the $(i+1)_{st}$ interval are a repetition of the last four coefficients in the i_{th} interval. Hence we may approximate the solution in the i_{th} interval as

$$U(z,t) = \sum_{k=1}^{8} C_{k+4(i-1)}(t) H_k(z), \tag{2.3}$$

where we have dropped the superscript i. The continuity of the basis functions across two successive interval is shown in figure 2

3. ORTHOGONAL COLLOCATION ON FINITE ELEMENTS

We consider the following fourth order nonlinear PDE which is known as the generalized Kuramoto Sivashinsky equation:

$$u_t + \varepsilon u u_x + \nu u_{xx} + \mu u_{xxx} + \delta u_{xxxx} = 0, \quad x \in [a,b], \quad t \geq 0 \tag{3.1}$$

where ε, ν, μ and δ are non-negative constants and the PDE is augmented with four boundary conditions at $x = a,\ x = b$ together with an initial condition at $t = 0$, which are appropriately defined. For the numerical solution of (3.1) we first apply the quasilinearization technique to linearize the PDE on $[t_j, t_{j+1}]$. After discretization in space, the collocation method using the trial solution (2.3) is applied on $[x_i, x_{i+1}]$, effectively known as collocation on finite elements.

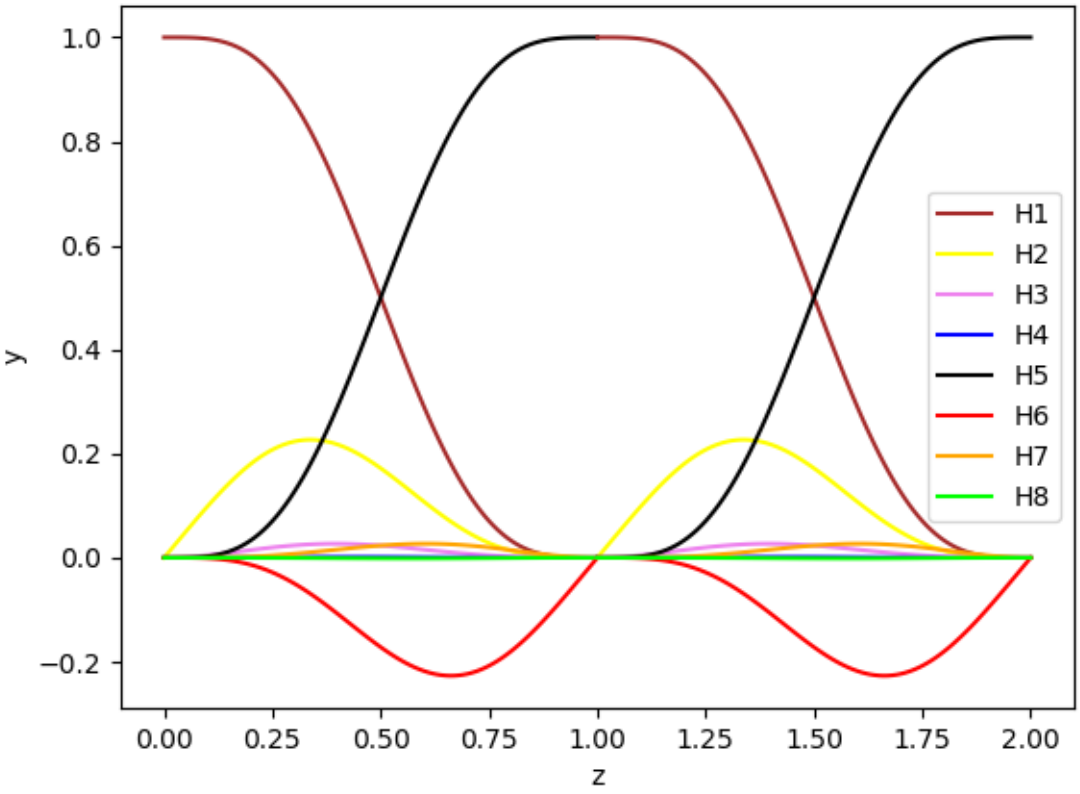

Figure 2: Basis functions $H_i(z)$ in the i_{th} and $(i+1)_{th}$

Equation (3.1) is integrated on $[t_j, t_{j+1}]$ using the trapezoidal rule, also known as the Crank-Nicholson Method [25], to yield the following numerical scheme:

$$\begin{aligned}&\left[1+\frac{\varepsilon\Delta t}{2}u_x(x,t_j)\right]u(x,t_{j+1})+\frac{\varepsilon\Delta t}{2}u(x,t_j)u_x(x,t_{j+1})+\nu\frac{\Delta t}{2}u_{xx}(x,t_{j+1})\\&+\mu\frac{\Delta t}{2}u_{xxx}(x,t_{j+1})+\delta\frac{\Delta t}{2}u_{xxxx}(x,t_{j+1})=u(x,t_j)-\nu\frac{\Delta t}{2}u_{xx}(x,t_j)\\&-\mu\frac{\Delta t}{2}u_{xxx}(x,t_j)-\delta\frac{\Delta t}{2}u_{xxxx}(x,t_j)\end{aligned}\tag{3.2}$$

Transforming to z and substituting (2.3) into (3.2), we get

$$\begin{aligned}&\sum_{k=1}^{8}\left(\left[1+\frac{\varepsilon\Delta t}{2h}\sum_{k=1}^{8}C_{k+4(i-1)}(t_j)H_k'(z)\right]H_k(z)+\left[\frac{\varepsilon\Delta t}{2h}\sum_{k=1}^{8}C_{k+4(i-1)}(t_j)H_k(z)\right]H_k'(z)\right.\\&\left.+v\frac{\Delta t}{2h^2}H_k''(z)+\mu\frac{\Delta t}{2h^3}H_k'''(z)+\delta\frac{\Delta t}{2h^4}H_k''''(z)\right)C_{k+4(i-1)}(t_{j+1})\\&=\sum_{k=1}^{8}\left[H_k(z)-v\frac{\Delta t}{2h^2}H_k''(z)\ -\mu\frac{\Delta t}{2h^3}H_k'''(z)-\delta\frac{\Delta t}{2h^4}H_k''''(z)\right]C_{k+4(i-1)}(t_j).\end{aligned}\tag{3.3}$$

We choose four collocation points in each subinterval and substitute into equation (3.3). The points are chosen as the Gauss points shifted to the interval $[0, 1]$ for optimal spatial error. Together with the four boundary conditions we obtain a $(4N + 4) \times (4N + 4)$ linear system of the form

$$M\mathbf{C}^{j+1} = B\mathbf{C}^{j}$$

where $\mathbf{C}^{j+1}$ is the vector of unknown coefficients at time t_{j+1}. We determine $\mathbf{C}^{0}$ from the initial condition

$$\begin{aligned} u(z, t_0) &= U(z, t_0) \\ &= \sum_{k=1}^{8} C_{k+4(i-1)}(t_0) H_k(z), \end{aligned} \tag{3.4}$$

by substituting the collocation points into equation (3.4) and solving the resulting linear system. The spatial error is $O(h^8)$ and is consistent with the work of [19]. As the Crank-Nicolson method is $O(dt^2)$ and the temporal order is not affected by the linearization, the method is overall $O(h^8 + dt^2)$. We confirm the spatial order by choosing $\Delta t = O(h^4)$ and using the following computation:

$$\text{order}^{\infty} = \frac{\ln\left(\frac{E^{N_1}}{E^{N_2}}\right)}{\ln\left(N_2/N_1\right)} \tag{3.5}$$

where $E^{N_1} = ||u(x, t) - U(x, t)||_{\infty}$ using N_1 spatial intervals and E^{N_2} is similarly defined.

4. NUMERICAL EXAMPLES AND SIMULATIONS

For numerical comparison we define the global relative error (GRE) [14]

$$GRE = \frac{\sum_{i=1}^{N+1} |u(x_i, t) - U(x_i, t)|}{\sum_{i=1}^{N+1} |u(x_i, t)|}$$

where $U(x_i, t)$ denotes the numerical solution and $u(x_i, t)$ denotes the exact solution. As there is super convergence at the nodes x_i of $O(h^{2r})$, where r is the number of Gauss collocation points per subinterval [19], it may be shown that the GRE can also be used to estimate the order by

$$\text{order}^{GRE} = \frac{\ln\left(\frac{GRE^{N_1}}{GRE^{N_2}}\right)}{\ln\left(N_2/N_1\right)} \tag{4.1}$$

where GRE^{N_1} refers to the GRE using N_1 spatial subintervals and GRE^{N_2} is similarly defined.
Example 1. We consider the Kuramoto Sivashinsky equation which is obtained by setting $\mu = 0$ in (3.1).

We set $\varepsilon = \nu = \delta = 1$ in (3.1) and take $x \in [-30, 30]$. The exact solution is given by [14]

$$u(x, t) = a_1 + \frac{15}{19}\sqrt{\frac{11}{19}}[-9\tanh(a_2(x - a_1 t - x_0)) + 11\tanh^3(a_2(x - a_1 t - x_0))] \tag{4.2}$$

$a_1 = 5, a_2 = \frac{1}{2}\sqrt{\frac{11}{19}}, x_0 = -12$. The initial condition and Dirichlet boundary conditions are extracted from the exact solution by setting $t = 0$ and $x = -30,\ x = 30$, respectively, in (4.2). Since we have a fourth order derivative in (3.1) we require two additional boundary conditions which are taken as

$$u_{xx}(-30, t) = u_{xx}(30, t) = 0.$$

t	1	2	3	4
GRE^1	1.2335×10^{-4}	1.6780×10^{-4}	2.0791×10^{-4}	2.5018×10^{-4}
GRE^2	6.6956×10^{-5}	9.6417×10^{-5}	1.0947×10^{-4}	1.2600×10^{-4}
order^{GRE}	2.123	1.926	2.229	2.384

Table 4.1: [15] *GRE errors and order for* $t = 1, 2, 3, 4$*:* GRE^1 *and* GRE^2 *correspond to* $N_1 = 300,\ N_2 = 400$*, respectively.*

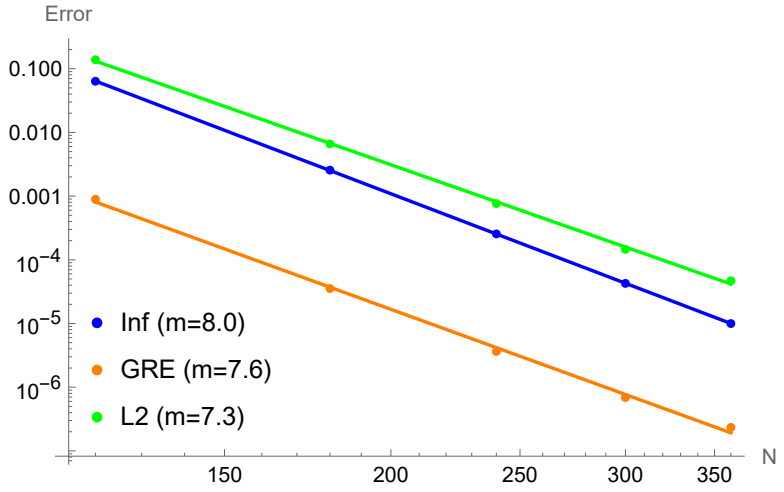

Figure 3: Order for various norms $t = 1$

t	1	2	3	4
GRE (Lai&Ma [14])	6.7923×10^{-4}	1.1503×10^{-3}	1.5941×10^{-3}	2.0075×10^{-3}
GRE^1 (Present Method)	3.5460×10^{-5}	6.5605×10^{-5}	9.4498×10^{-5}	1.2117×10^{-4}

Table 4.2: GRE errors for various t *values.*

The problem above was solved in [15] using Quintic B-splines and Crank Nicolson method. It is observed in table 4.1 that their scheme has order approximately equal to two. We will demonstrate that the method proposed here has a much higher order of eight. In Figure 4 we illustrate a 3D plot of the solution using $N = 300$. It is observed that the solution represents a single antisymmetric wave traveling to the right (this is more clearly visible in the right picture which shows the top view). Table 4.2 gives the GRE for various t values using $\Delta t = (\Delta x)^4$. In Table 4.2 we compare the results obtained by Lai and Ma [14] (GRE) with the results obtained using the present method (GRE^1). In the paper of Lai and Ma [14] they computed the solution using $N = 600,\ \Delta x = 1/10,\ \Delta t = (\Delta x)^4$, (a grid of size 6×10^6) and obtained the GRE shown in Table 4.2. Using $N = 180,\ \Delta x = 1/3,\ \Delta t = (\Delta x)^4$ (a grid of size 43740) we obtained a more accurate solution for a considerably smaller grid. Moreover, in Figure 3 we display the errors for various norms on a Log-log scale. It is clearly observed that the GRE error using $N = 360$ is much smaller than that obtained by Lai and Ma [14]. The value of m represents the slope of a linear fit of the data and we observe that the order of the method is 8 as predicted by the theory [19].

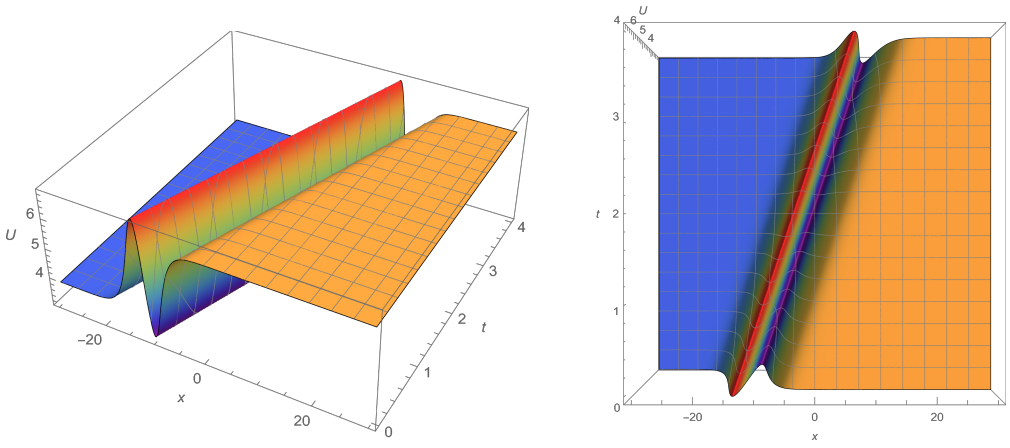

Figure 4: Left panel: 3D surface plot with $N = 300$. Right panel: Top view

t	6	8	10	12
GRE (Lai&Ma [14])	7.8808×10^{-6}	9.5324×10^{-6}	1.0891×10^{-5}	1.1793×10^{-5}
GRE^1 (Present Method)	1.8017×10^{-6}	2.3418×10^{-6}	2.8795×10^{-6}	6.2398×10^{-6}

Table 4.3: GRE error for $x \in [-50, 50]$, $t = 6, 8, 10, 12$ values, $N = 300$.

Example 2. As a second example we consider by setting $\mu = 0$, $\varepsilon = \delta = 1$ and $\nu = -1$ in (3.1) and take $x \in [-50, 50]$. The exact solution is given by

$$u(x,t) = b + \frac{15}{19\sqrt{19}}\left[-3\tanh(k(x - bt - x_0)) + \tanh^3(k(x - bt - x_0))\right] \tag{4.3}$$

$b = 5, k = \frac{1}{2\sqrt{19}}, x_0 = -25$

The initial condition and Dirichlet boundary conditions are extracted from the exact solution by setting $t = 0$ and $x = -50,\ x = 50$, respectively, in (4.3) and the additional boundary conditions:

$$u_{xx}(-50, t) = u_{xx}(50, t) = 0.$$

In table 4.3 we tabulated the results of the method given in [14] who used a computational grid of size 10^7 and the present method for $t = 6, 8, 10, 12$. The GRE^1 obtained using the present method was calculated using using $N = 300$, which corresponds to a computational grid of size 24300. Once again it is observed that the results obtained using the present method is superior to that obtained in [14]. Figure 5 gives the order computed in various norms on a Log-log scale and confirms the expected order of 8. Figure 6 illustrates a 3D surface plot of the solution.

Example 3. In this example taken from [14] we take $\varepsilon = 1,\ \nu = 1,\ \mu = 4,\ \delta = 1$ and take $a = -30,\ b = 30$ in (3.1). This case corresponds to the generalized Kuramoto Sivashinsky equation. The exact solution is given by

$$u(x,t) = b + 9 - 15\left(\tanh(k(x - bt - x_0)) + \tanh^2(k(x - bt - x_0)) - \tanh^3(k(x - bt - x_0))\right),$$

where $b = 6,\ k = \dfrac{1}{2},\ x_0 = -10$. The initial and boundary conditions are chosen as in the previous example.

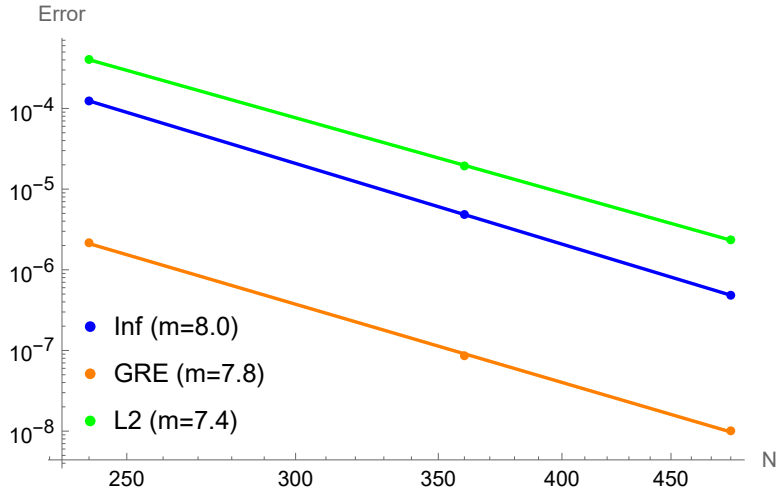

Figure 5: Order for various norms $t = 1$

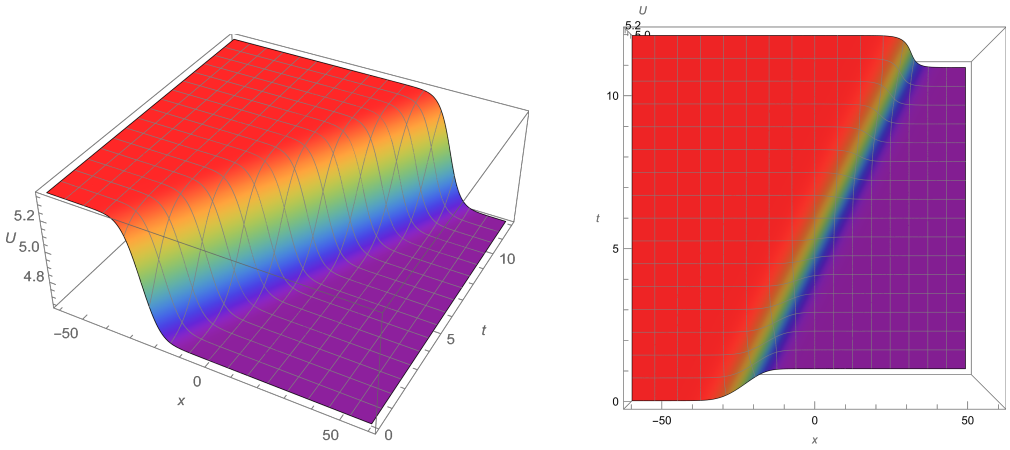

Figure 6: Left panel: 3D surface plot $x \in [-60, 60]$ with $N = 300$. Right panel: Top View.

t	1	2	3	4
GRE (Lai&Ma [14])	2.5945×10^{-2}	2.7959×10^{-2}	2.6701×10^{-2}	3.5172×10^{-2}
GRE^1 (Present Method)	2.0599×10^{-3}	3.1221×10^{-3}	3.3803×10^{-3}	3.0072×10^{-3}

Table 4.4: GRE error for various t values and $N = 180$.

In table 4.4 we tabulated the results of the method given in [14] who used a computational grid of size 6×10^6 and the present method for $t = 1, 2, 3, 4$. The GRE^1 obtained using the present method was calculated using using $N = 180$, which corresponds to a computational grid of size 14580. Once again it is observed that the results obtained using the present method is superior to that obtained in [14]. Figure 7 gives the order computed in various norms on a Log-log scale and confirms the expected order of 8. Figure 8 illustrates a 3D surface plot of the solution.

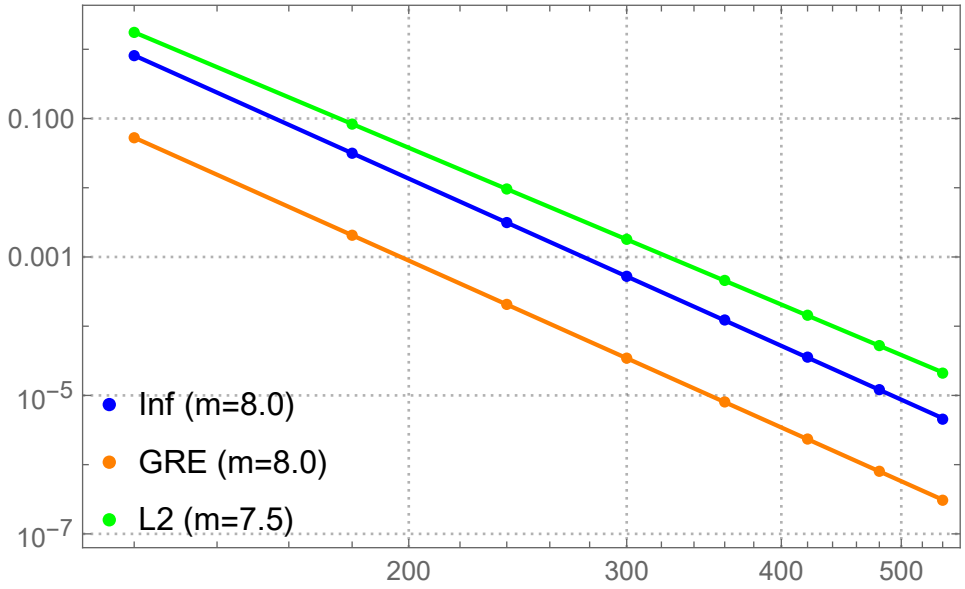

Figure 7: Order for various norms $t = 1$

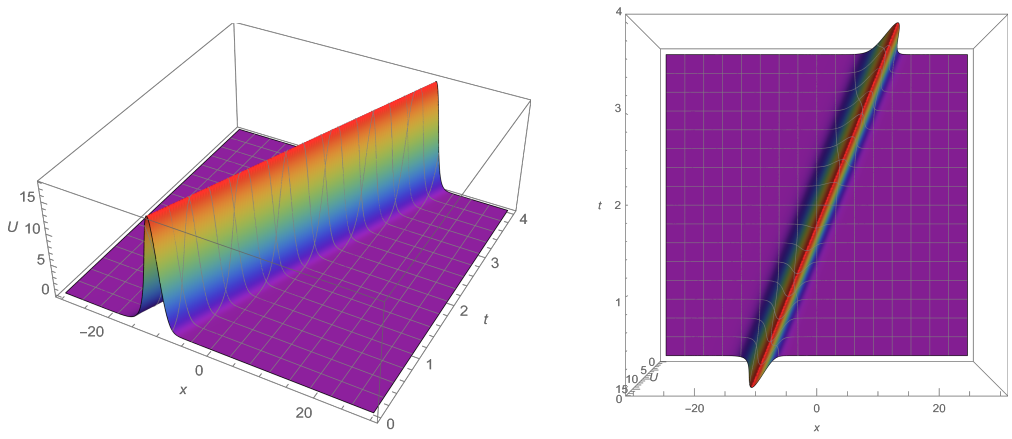

Figure 8: Left panel: $3D$ *surface plot with* $N = 300$*. Right panel: Top view*

Example 4. In our final example we consider a scenario in which (3.1) is used as a model to simulate chaotic solutions . We consider solving (3.1) with the same parameters as defined in Example 1, but with the initial condition chosen as the Gausssian function (see [15] and references therin)

$$u(x, 0) = e^{-x^2},$$

and homogeneous boundary conditions

$$\begin{aligned} u(-30, t) &= u(30, t) = 0 \\ u_{xx}(-30, t) &= u_{xx}(30, t) = 0. \end{aligned}$$

The computations are performed using $N = 300$, $\Delta t = 0.01$, and $T_{final} = 20s$. Figure 9 represents a $3D$ surface plot of the solution. It is observed that the solution is not a traveling wave but resembles the solution of a chaotic system. The right plot gives the top view and

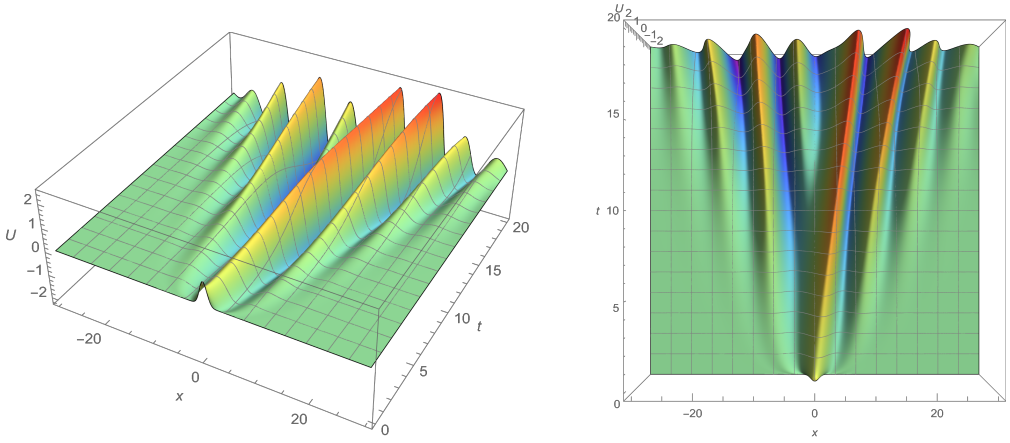

Figure 9: Left panel: $3D$ surface plot with $N = 300,\ \Delta t = 0.01$. Right panel: Top view

clearly shows how a simple initial condition evolves into a solution with a more complicated behaviour.

5. CONCLUSION

In this paper we have derived the C^3 heptic Hermite basis and used it to develop the OCFE method to solve the generalised Kuramoto equation. The gKSe describe many physical phenomena in the nonlinear sciences. The use of Gauss points as collocation points yields superconvergence at selected points in the spatial domain. It is demonstrated that the spatial order of the method is eight and that the current numerical method is more appealing than the eminent works presented in [12, 13, 15, 14]. A complete set of numerical examples and simulations are presented which demonstrate that the current method is suitable for handling various situations characterized by the solution of the gKSe, such as traveling waves, solitons and chaotic solutions.

REFERENCES

[1] C.D. BRUMMIT and J. SPROTT, A search for the simplest chaotic partial differential equation, *Phys Lett A.*, **58** (2013), pp. 2717–2721.

[2] J.M. HYMAN and B. NICOLAENKO, The Kuramoto-Sivashinsky equation: A bridge between PDE's and dynamical systems, *Physica D.*, **18** (1986), No. 1-3, pp. 113–126.

[3] D.T. PAPAGEORGIOU and Y.S. SMYRLIS, The Route to chaos for the Kuramoto-Sivashinsky equation, *Theor Comput Fluid Dyn.*, **3** (1991), No. 1, pp. 15-42.

[4] Y. KURAMOTO and T. TSUZUKI, Persistent propagation of concentration waves in dissipative media far from thermal equilibrium, *Prog Theor Phys.*, **55** (1976), No. 2, pp. 356–369.

[5] G.I. SIVASHINSKY, Instabilities, pattern formation, and turbulence in flames, *Annu Rev Fluid Mech.*, **15** (1983), No. 1, pp. 179–199.

[6] G.I. SIVASHINSKY and D. MICHELSON, On irregular wavy flow of a liquid film down a vertical plane, *Prog Theor Phys*, **63** (1980), pp. 2112–2114.

[7] U. THIELE and E. KNOBLOCH, Thin liquid films on a slightly inclined heated plate, *Physica D*, **190** (2004), No. 3-4, pp. 213–248.

[8] P.M. TREVELYAN and S. KALLIADASIS, Dynamics of a reactive falling film at large Peclet numbers. I. Long-wave approximation, *Phys Fluids*, **16** (2004), No. 8, pp. 3191–3208.

[9] B.I. COHEN and J. KROMMES and W. TANG and M. ROSENBLUTH, Non-linear saturation of the dissipative trapped-ion mode by mode coupling, *Nuclear Fusion*, **16** (1976), No. 6, pp. 971–992.

[10] M. SATO and M. UWAHA, Step bunching as formation of Soliton-like pulses in Benney equation, *Eurphysics Letters*, **32** (1995), No. 8, pp. 639.

[11] B. NICOLAENKO, B. SCHEURER and R. TEMAM, Some global dynamical properties of the Kuramoto-Sivashinsky equation: Nonlinear stability and attractors, *Physica D*, **16** (1985), No. 2, pp. 155–183.

[12] G. D. AKRIVIS, Finite difference discretization of the Kuramoto-Sivashinsky equation, *Numerische Mathemamatik*, **63** (1992), pp. 1–11.

[13] G. D. AKRIVIS, High-order finite element methods for the Kuramoto-Sivashinsky equation, *Rairo-Mathematical Modelling and Numerical Analysis*, **30** (1996), No. 2, pp. 157–183.

[14] H. LAI and C. MA, Lattice Boltzmann method for the generalized Kuramoto-Sivashinsky equation, *Physica A: Statistical Mechanics and Its Applications*, **388** (2009), No. 8, pp. 1405–1412.

[15] R.C. MITTAL and G. ARORA, Quintic B-spline collocation method for numerical solution of the Kuramoto-Sivashinsky equation, *Commun Nonlinear Sci Numer Simulat.*, **15** (2010), pp. 2798–2808.

[16] S.S. SOLIMAN, Collocation solution of the Korteweg-de Vries equation using septic splines, *International Journal of Computer Mathematics.*, **81** (2004), No. 3, pp. 325–331.

[17] S.I. ZAKI, A Quantic B-spline finite elements scheme for the KDVB equation, *Computer Method in Applied Mechanics and Engineering.*, (2000), pp. 121–134.

[18] A.K. MITTAL, I.A. GANAIE, V.K. KUKREJA, N. PARUMASUR and P. SINGH, Solution of diffusion-dispersion models using a computationally efficient technique of orthogonal collocation on finite elements with cubic Hermite as basis, *Computers and Chemical Engineering*, **58** (2013), pp. 203–210.

[19] C. de BOOR, B. SWARTZ, Collocation at Gaussian Points, *SIAM J. Numerical Analysis*, **10** (1973), No. 4, pp. 582–606.

[20] S. ARORA, S.S. DHALIWAL and V.K. KUKREJA, Solution of two point boundary value problems using orthogonal collocation on Finite Elements, *Applied Mathematics and Computation*, **171** (2005), No. 1, pp. 358–370.

[21] S. ARORA, R. JAINA and V.K. KUKREJA, Solution of Benjamin-Bona-Mahony-Burgers equation using collocation method with Quintic Hermite splines, *Applied Numerical Mathematics*, **154** (2020), pp. 1âĂŞ16.

[22] B.A. FINLAYSON, Orthogonal collocation on Finite elements - Progress and Potential, *Mathematics and Computers in Simulation*, **22** (1980), pp. 11–17.

[23] I.A. GANAIE and S. ARORA and V.K. KUKREJA, Cubic Hermite collocation solution of Kuramoto-Sivashinskye equation, *International Journal of Computer Mathematics*, **93** (2016), No. 1, pp. 223–235.

[24] A.V. MANICKAM, K.M. MOUDGALYA and A.K. PANI, Second-order splitting combined with orthogonal cubic spline collocation method for the Kuramoto-Sivashinsky equation, *Computers Math. Applic.*, **35** (1998), No. 6, pp. 5–25.

[25] S.G. RUBIN and R.A. GRAVES, A cubic spline approximation for problems in fluid mechanics, *NASA TR R-436, Washington, DC,* , (1975), pp. 1–91.

[26] N. J. ZABUSKY and M. D. KRUSKAL (1965), Interaction of solitons in a collisionless plasma and the recurrence of initial states, *Phys. Rev. Lett.*, **15** (1965), pp. 240–243.